International Journal of Computer Information Systems and Industrial Management Applications
ISSN 2150-7988 Volume 18(16s) 2026 pp. 707-719
https://doi.org/10.70917/ijcisim-2026-4601
Article

Asymptotic Performance Analysis of Diversity-Enabled Finite-Block length Systems over the Family of Single and Double Shadowed κ-μ Fading Channels

Ankit Jain[1,2], Imran Ullah Khan[1], Puspraj Singh Chauhan[2,3*], Utkarsh Pandey[2], Vimal Bhatia[3]

[1]Department of ECE, Integral University, Lucknow, India.
[2]Department of ECE, Pranveer Singh Institute of Technology, Kanpur, India.
[3]Department of Electrical Engineering, IIT, Indore, India.
*Corresponding author(s). E-mail(s): puspraj.chauhan@{gmail.com,iit.ac.in};
Contributing authors: ankit2483jain@gmail.com; iukhan@iul.ac.in; utkarsh.pandey08@gmail.com; vbhatia@iiti.ac.in

Abstract: . The analytical complexity inherent in the family of κ−μ/shadowed fading family often restricts its practical applicability in diversity-based systems and complicates the direct interpretation of performance metrics for wireless communication systems. To overcome these challenges, this work proposes a unified and simplified asymptotic framework for the family of κ−μ/shadowed fading models, accommodating both single and double shadowing scenarios with diversity. Initially, we derive the fundamental probability density function expressions for single-input and single-output (SISO) system than extended it with employing selection combining (SC) schemes. Building on this, asymptotic analysis of short-packet communication performance metrics, specifically average block error rate and delay outage rate, is presented. The framework is further extended to quantify diversity and signal-to-noise ratio (SNR) gains. At last, we validated the analytical finding with Monte-Carlo simulations and found these results to be in close-agreement, confirming the accuracy of the provided formulations.
Keywords: Bit Error Rate, Diversity, Fading, Gaussian Noise.

1. Introduction

In view of the development of 5G and future beyond 5G networks, mobile network operators claim enhancements in management of networks, reductions in latency, high data rate, and improved coverage of services in areas that were not accessible earlier [1], [2]. Of the above criteria, the problem of latency has gained paramount importance in various communication applications, such as Internet of Things, machine to machine communication, device to device communication, and other sophisticated applications that cannot tolerate latency [3]. In order to meet these demanding specifications, new communication techniques involving the use of short packets instead of traditional long packets have received much consideration. This technique is known as short packet communication (SPC) [3]. Due to the demand for ultrareliable low latency communication (URLLC) depending upon small data packets and constrained latency requirement for mission-critical services, the importance of 6G wireless networks has increased [4], [5]. Here SPC becomes a crucial criterion compared to the traditional Shannon capacity since it does not meet the strict delay requirements [6], [7]. Since wireless channels are unpredictable by their nature, this results in poor signal-to-noise ratio (SNR), and poor performance overall. Although proper choice of the right transmission scheme helps to cope with problems related to latency, this problem is still present. Hence, failure to take into account channel behavior may cause poor performance.

1.1 Literature Review

In the existing literature, various kinds of fading channel models have been developed, including those that represent conventional or classic fading models and generalized fading models that are suitable for different wireless system settings. The key feature of these generalized models is their versatility, as they allow describing different propagation environments while maintaining the properties and behavior of the conventional models on which they are based [8]. Among all channel models, one should pay special attention to the κ-μ/shadowed (KMS) model as a very versatile composite channel model. This model is able to generalize several types of classic fading situations and give a broader description of shadowed/Rician situations as well. Due to the high level of its versatility and the strong correspondence with the real-life situation, the KMS model has gained a lot of popularity among models of wireless channels. It has found numerous applications in a variety of wireless communications such as land-mobile satellite channels, underwater acoustic channels, body-centric networks, and vehicular communication channels [9-12].

In [13], Simmons et al conducted a comprehensive study of the family of KMS fading. The study focuses on investigating the effect of different shadowing mechanisms on the dominant and the scattered components of the classical κ-μ fading model. To understand the multitude of the possible real-world situations, the authors suggest a physical approach for modeling a wireless propagation channel depending on whether the shadowing mechanism can have one or several stages. Therefore, the framework allows modeling of the propagation conditions when the different signal components are affected by distinct environmental obstacles and channel variations. For the single-shadowing case, the analysis involves consideration of three models depending on which components of the κ-μ signal are shadowed. According to the Type-I single-shadowing case, the shadowing mechanism affects only the dominant component of the signal. Such model can be applied to describe the propagation environments when the line-of-sight propagation and other specular components are shadowed while the scattered multipath components stay unaffected. On the contrary, the Type-II single-shadowing model describes the shadowing of the scattered component. Such scenario can be used in the cases when the diffuse multipath components are subjected to variations because of the changes in the propagation environment while the dominant signal component stays the same. Finally, the Type-III single-shadowing model presents a more general propagation condition when the dominant and scattered components are shadowed.

The study also expanded the framework of single-shadowing models by presenting a set of double-shadowing models that can be used for modeling situations in which either two shadowing phenomena occur sequentially or simultaneously. There were three possible forms of double-shadowing models were considered. In the Type-I double-shadowing mechanism, the dominant part of the signal encounters a primary shadowing phenomenon and further faces a secondary multiplicative shadowing effect. This mechanism makes it possible for the proposed model to capture the environment where the dominant part of the signal is attenuated initially and then faces another independent fluctuation of either large scale or medium scale. In the case of Type-II double-shadowing, the dominant component of the signal faces two independent shadowing effects. In this way, the model becomes flexible to capture the channel environment in which the dominant signal experiences multiple attenuations or fluctuation. The Type-III double-shadowing model takes care of a more generalized channel environment than the other two forms. In this case, the scattered component of the κ-μ fading signal encounters shadowing, but at the same time, the root mean square (RMS) value corresponding to both the dominant and the scattered components of the signal suffers from another independent shadowing phenomenon. The mechanism covers the situation when the fluctuations exist not only in the diffuse multipath component of the signal but also in the total signal power level. In order to describe the statistical nature of such diverse shadowing scenarios, the shadowing was described through either the Nakagami-(m) distribution or a combination of the Nakagami-(m) and inverse-Nakagami-(m) distributions. Such distributions offer great modeling capability and allow for the ensuing KMS models to cover a wide range of fading and shadowing scenarios. The physical meanings of the different shadowing schemes along with representative wireless communication scenarios that can lead to such KMS models are described in [13, Tables 1 and 2].

Based on this prior work, the researchers in [14] analyzed the statistical and performance properties of a single KMS fading model with additive Laplacian noise. Specifically, they developed a closed-form formula for the bit error rate (BER) considering that the noise is not Gaussian. They also found the asymptotic formula for the probability density function (PDF) in the vicinity of the origin. The PDF at the origin was used to derive simplified asymptotic performance expressions.

In line with the above, the type-I double KMS distribution has been studied extensively in [15]–[18], where various performance measures related to communications have been analyzed. Both the exact and asymptotic representations of these measures have been obtained to ensure an all-around analysis of the behavior of the system under consideration under various conditions. For example, the effective capacity of wireless systems using double KMS fading channels has been studied in [16], giving the performance measure that allows estimating the sensitivity of the system regarding delays during the transmission process. Outage performance has been studied in [17], which gives information on the probability that the quality of the instantaneous channel is less than a given threshold. Besides, asymptotic representations of the average symbol error probability (ASEP) have been provided in [18], providing useful information on the high-SNR performance and diversity properties of the system. In addition to these traditional performance measures in communications, detection performance measures such as the probability of detection and average area under the receiver operating characteristic curve have been analyzed. Moreover, the investigation was extended by incorporating three commonly used diversity combining schemes: maximal-ratio combining (MRC), equal-gain combining (EGC), and selection combining (SC). Overall, the existing studies provide valuable analytical results for single and double KMS fading models; however, the majority of the reported investigations remain focused on specific KMS configurations and selected performance metrics.

1.2 Motivation and Contributions

The probability density functions (PDFs) developed in [13] are given in the form of infinite series, except for those for the single and double KMS Type-I fading conditions. Although these expressions give a mathematically general description of the fading channels being investigated, the fact that these expressions contain infinite series makes the analysis quite complex, especially when diversity reception is taken into account. This makes it hard to find tractable expressions for PDFs for such diversity systems, despite the fact that diversity is commonly used as a method to combat the adverse effect of multipath fading. Furthermore, the complex mathematical expressions involved might hide any clear relation between performance measures of the system and fading conditions. This limitation makes it difficult to clearly identify the influence of channel characteristics, such as the multipath and shadowing parameters, on the overall system behavior. In order to circumvent these difficulties, the framework offered in [19] offers an easier approach, especially in the case of high transmit powers or high SNR. Utilizing the asymptotic properties of the underlying fading distribution, the approach circumvents the need for direct evaluation of complex infinite series expressions. However, more significantly, the resultant asymptotic formulas give us valuable physical understanding of the working of the communication system in question. This helps to interpret how the fading parameters affect various metrics and to characterize important parameters, including diversity order and parameters governing the performance. In addition, since the expressions thus obtained are compact in form, the task of analysis is made easier, and efficient parametric studies become possible. Such simplified formulas can also be of help in the design of practical systems, where the choice of appropriate channel and receiver parameters becomes necessary in order to achieve good performance.

However, despite the remarkable progress that has been made, the existing literature concerning KMS fading channels largely focuses on the performance of long packet communication systems. While these studies can be quite useful in conventional wireless communications, they do not adequately reflect the characteristics of URLLC. As the name implies, in URLLC systems, information is transferred via short packets. In such cases, the assumptions about the performance of traditional wireless systems based on long codewords may not hold anymore. Thus, studying the performance of short packet communication systems through generalized fading environments becomes especially important for the design of 5G and beyond wireless communication systems. The literature concerning asymptotic performance analysis of the KMS family of models is relatively scarce. For instance, the paper [14] analyzed the asymptotic bit error rate of single-antenna point-to-point communication under Laplacian noise conditions. On the other hand, the papers [9], [12], [16], and [18] focus on Type-I single and double shadowed κ-μ fading environments. There are several important questions that remain open, for instance, asymptotic performance analysis of receiver diversity systems and performance of short packet transmissions in more general single and double shadowed κ-μ fading environments.

Inspired from the mentioned limitations in the literature, the current work employs SC at the receiver (Rx) side to utilize the advantage of spatial diversity and improve the received SNR. With diversity combining, one may be able to overcome the effect of deep fading and thereby increase the reliability of the system. Besides, the current work evaluates the performance of short packet transmission in κ-μ fading channel with and without shadowing. Such kind of performance evaluation would provide a better understanding regarding the performance of the wireless systems which should be evaluated according to stricter reliability and delay constraints in future 5G networks and beyond. The following are the main contributions of this work:

- In this paper, the expression of PDF near origin of a SISO channel has been obtained while applying SC diversity technique. Such analysis is performed considering two different shadowing conditions. The first shadowing condition is with a single KMS model considering the Type-I, Type-II, and Type-III shadowing, while the other is with a double KMS Type-I, Type-II, and Type-III shadowing. Apart from getting the near origin PDF expressions for each of these cases, an unified expression has been obtained for all the shadowing cases.

- Utilizing the above-derived origin PDF formulas, an asymptotic analysis framework is formulated in order to study two essential performance metrics, which include the block error rate (BLER) and the delay outage rate (DOR). As a result of the introduced analysis framework, the high-SNR characteristics of the above-mentioned metrics can be analyzed and studied in an overall manner. In addition, the dependencies between the diversity gain and SNR gain with respect to the BLER and DOR performance can be studied. Based on the above-mentioned analysis, one can understand the effect of the diversity scheme, shadowing model, and other system parameters on the reliability and delay performance of the system.
- The accuracy of the developed asymptotic expressions is verified through extensive Monte Carlo simulations. The analytical results exhibit a close agreement with the corresponding simulation outcomes, particularly in the high-transmit-power region. This consistency confirms the validity of the proposed asymptotic framework and demonstrates its effectiveness in accurately predicting the system performance under different diversity and shadowing conditions.

2. Preliminaries

2.1 System Model

In the present study, we consider a point-to-multipoint wireless communication system wherein the transmitter (Tx) consists of one antenna and Rx uses multiple antennas to ensure better reception of the signal. Multiple antennas used at the receiver help in exploiting the spatial diversity of the system in order to minimize the effect of the channel fading and achieve high communication performance. To make full use of the diversity branches without increasing the implementation complexity too much, the receiver uses SC technique. In the SC process, the instantaneous SNR of the individual (L) diversity branches is estimated and then the branch having the highest value of instantaneous SNR is chosen for the signal detection purpose. As a result, the diversity gain is achieved without performing coherent combination of all the branches. The received signal for the (l)-th diversity branch under the aforementioned system model can be written as follows:

$$\mathcal{R}_l = \mathcal{H}_l \mathcal{S} + \mathcal{N}_l \quad \ldots\ldots\ldots\ldots\ldots\ldots\ldots (1)$$

where H_l represents the coefficient of the transmitted channel, $\mathcal{S}$ signifies the data transmitted over the channel, and $\mathcal{N}_l$ denotes the noise, which is complex Gaussian in nature with mean zero and unity variance.

2.2 Fading Characteristic

In this section, the derivation of origin PDF for the generalized KMS fading model under diversity combining scheme will be discussed. At first, the derivation of the origin PDF for a single KMS fading channel will be discussed. This is because the origin PDF of a single KMS fading channel forms the foundation in evaluating the performance of the system. Following that, the analysis is expanded into double-shadowed KMS fading model where there is another additional source of randomness in the system. Consequently, there are higher variations of the fading process, hence the necessity to employ a more generalized framework to model the statistics of the fading process. In addition, the origin PDF expression for MRC and SC schemes at the Rx will be derived.

2.2.1 Single Shadowed $\boldsymbol{\kappa - \mu}$ Fading

The unified origin PDF expression has already been proposed in [14]

$$f_\gamma(\gamma)^0 \simeq \frac{\hat{R}}{\bar{\gamma}^\mu} \gamma^{\mu-1} \quad \ldots\ldots\ldots\ldots\ldots\ldots\ldots (2)$$

where $\hat{R}$ represents parameters for different shadowing types as illustrated in [14, Table 3] and $\bar{\gamma}$ is the average SNR of the distribution. For the sake of completeness, the table is reproduced here as illustrated by Table 1, where μ, κ, and m are the number of multipath clusters, the power ratio of dominant to scattered components, and the Nakagami-m shape parameter.

Table 1: Parameters for origin single KMS family PDFs

Fading Types	$\widehat{\boldsymbol{R}}$
Single KMS Type-I	$\frac{\mu^{\mu} m^{m}(1+\kappa)^{\mu}}{\Gamma(\mu)(m+\mu\kappa)^{m}}$
Single KMS Type-II	$\frac{2\mu^{\mu} m^{m}(1+\kappa)^{\mu}}{\Gamma(\mu)\Gamma(m)}\left(\frac{\mu\kappa}{m}\right)^{\frac{m-\mu}{2}} K_{m-\mu}\left(2\sqrt{m\mu\kappa}\right)$
Single KMS Type-III	$\frac{\mu^{\mu} m^{m}(1+\kappa)^{\mu}\Gamma(m-\mu)}{\Gamma(\mu)\Gamma(m)e^{\mu\kappa} m^{m-\mu}}$

2.2.2 Double Shadowed $\kappa-\mu$ Fading

The origin PDF representation for the double KMS Type-I scheme is presented in reference [19], but unfortunately, the corresponding origin PDF representations for the shadowing types II and III have not been presented there. This shortcoming is overcome here by presenting an extended PDF approach which accommodates the three different types of shadowing in one single model. In double shadowing model, the Nakagami-(m) and inverse Nakagami-(m) distributions are utilized as the distributions representing the shadowing effects, and are given as

$$f_Z(z)=\frac{(m_r-1)^{m_r}}{\Gamma(m_r)z^{m_r+1}}e^{-\frac{(m_r-1)}{z}} \quad\ldots\ldots\ldots\ldots\ldots\ldots\ldots (3)$$

where $\Gamma(.)$ is the Gamma function.

2.2.2.1 Double Shadowed κ − μ Type-I Fading

Through the use of the PDF stated in (2) along with the corresponding Type-I parameters specified in Table I, the conditional PDF conditioned on the shadowing parameter (Z) is presented below:

$$f_{\gamma|Z}(\gamma)^0 \simeq \frac{\mu^{\mu} m^{m}(1+\kappa)^{\mu}}{\Gamma(\mu)(m+\mu\kappa)^{m}(z\bar{\gamma})^{\mu}}\gamma^{\mu-1} \quad\ldots\ldots\ldots\ldots\ldots\ldots\ldots (4)$$

By substituting (4) with (3) into the definition $f_\gamma(\gamma)=\int_0^\infty f_{\gamma|Z}(\gamma|z)f_Z(z)dz$ as stated in [15, Eq. (3)], where $f_{\gamma|Z}(\gamma|z)$ is the SNR PDF $f_\gamma(\gamma)$ conditioned over the shadowing variavle Z, the integral can be simplified through the change of variables $\frac{1}{z}=t$. Employing this transformation together with the aid of [20, Eq. (3.381.4))], enables the closed-form solution for the integral. Consequently, the origin PDF corresponding to double KMS Type-I is obtained in compact form as given by

$$f_\gamma(\gamma)\simeq\frac{\mu^{\mu} m^{m}(1+\kappa)^{\mu}\Gamma(m_r+\mu)}{\Gamma(\mu)\Gamma(m_r)(m+\mu\kappa)^{m}(m_r-1)^{\mu}}\frac{\gamma^{\mu-1}}{\bar{\gamma}^{\mu}} \quad\ldots\ldots\ldots\ldots\ldots (5)$$

2.2.2.2 Double Shadowed κ − μ Type-II Fading

In the double KMS Type-II model of fading, the dominant signal and the diffuse multipath signals both undergo independent shadowing. The dominant signal is modeled through the use of Nakagami-(m), while the scattered multipath signal is modeled through the use of inverse Nakagami-(m). With such consideration made on the basis of the shadowing process undergone, the near-origin PDF of the κ-μ fading channel is conditioned on the corresponding shadowing parameter as follows:

$$f_{\gamma|\zeta,\xi}(\gamma;\zeta,\xi)\simeq\frac{\mu^{\mu}(1+\kappa)^{\mu}\gamma^{\mu-1}}{\Gamma(\mu)\zeta^{2\mu}\bar{\gamma}^{\mu}}e^{-\frac{\xi^2\mu\kappa}{\zeta^2}} \quad\ldots\ldots\ldots\ldots\ldots\ldots\ldots\ldots (6)$$

where ξ, and ζ denotes Nakagami-m and inverse Nakagami-m random variables, with PDF

$$f_\zeta(\zeta)=\frac{2(m_r-1)^{m_r}}{\Gamma(m_r)\zeta^{2m_r+1}}e^{-\frac{(m_r-1)}{\zeta^2}} \quad\ldots\ldots\ldots\ldots\ldots\ldots\ldots\ldots (7)$$

$$f_\xi(\xi)=\frac{2m^m}{\Gamma(\xi)}\xi^{2m-1}e^{-m\xi^2} \quad\ldots\ldots\ldots\ldots\ldots\ldots\ldots\ldots\ldots (8)$$

On averaging the conditional PDF given by (6) with (7) and (8), we get

$$f_\gamma(\gamma) \simeq \frac{4m^m(m_r-1)^{m_r}}{\Gamma(m)\Gamma(m_r)}\frac{\mu^\mu(1+\kappa)^\mu\gamma^{\mu-1}}{\Gamma(\mu)\bar{\gamma}^\mu}\int_0^\infty\int_0^\infty \frac{\xi^{2m-1}}{\zeta^{2m_r+2\mu+1}} e^{-\frac{\xi^2\mu\kappa}{\zeta^2}} e^{-\frac{(m_r-1)}{\zeta^2}} e^{-m\xi^2} d\zeta d\xi \text{ .... (9)}$$

Setting $\xi^2 = t$ and utilizing the relation [20, Eq. (3.381.4)], (9) results into

$$f_\gamma(\gamma) \simeq \frac{2m^m(m_r-1)^{m_r}}{\Gamma(m_r)}\frac{\mu^\mu(1+\kappa)^\mu\gamma^{\mu-1}}{\Gamma(\mu)\bar{\gamma}^\mu}\int_0^\infty \frac{1}{\zeta^{2m_r+2\mu+1}\left(\frac{\mu\kappa}{\zeta^2}+m\right)^m} e^{-\frac{(m_r-1)}{\zeta^2}} d\zeta \text{ .... (10)}$$

Further, subsequently setting $\zeta^2 = r$ and $\frac{1}{r} = s$, and with the aid of [21, Eq. (2.3.6.9)], the previous integral simplifies to

$$f_\gamma(\gamma) \simeq \frac{\mu^\mu(1+\kappa)^\mu(m_r-1)^{m_r}\Gamma(\mu+m_r)}{\Gamma(\mu)\Gamma(m_r)\left(\frac{\mu\kappa}{m}\right)^{\mu+m}} \Psi\left(\mu+m_r, \mu+m_r-m+1; (m_r-1)\frac{m}{\mu\kappa}\right)\frac{\gamma^{\mu-1}}{\bar{\gamma}^\mu} \text{ .... (11)}$$

where $\Psi(.)$ is the Tricomi confluent hypergeometric function [20, Eq. (9.211.4[8])].

2.2.2.3 Double Shadowed $\kappa-\mu$ Type-III Fading

In the double KMS Type-III model of fading, the scattered signal related to each multipath cluster will experience fluctuations. The fluctuations are mathematically described through the use of the inverse Nakagami-(m). Thus, the conditional PDF of the $\kappa-\mu$ fading model near the origin is as follows:

$$f_{\gamma|\zeta}(\gamma;\zeta) \simeq \frac{\mu^\mu(1+\kappa)^\mu\gamma^{\mu-1}}{\Gamma(\mu)\bar{\gamma}^\mu e^{\frac{\mu\kappa}{\zeta^2}}\zeta^{2\mu}} \text{ .... (12)}$$

Further on averaging (12) with (7), subsequently setting $\zeta^2 = t$ and $t = \frac{1}{s}$ and utilizing [20, Eq. (3.381.4)], one can get

$$f_\gamma(\gamma) \simeq \frac{\mu^\mu(1+\kappa)^\mu(m_r-1)^{m_r}\Gamma(m_r+\mu)}{\Gamma(m_r)\Gamma(\mu)(\mu\kappa+(m_r-1))^{m_r+\mu}}\frac{\gamma^{\mu-1}}{\bar{\gamma}^\mu} \text{ .... (13)}$$

In addition, the second round of shadowing, where the root mean square (rms) power of the scattered and dominant components is subjected to shadowing, modelled with Nakagami-m distribution. Then the PDF around the origin is obtained via

$$f_\gamma(\gamma) = \int_0^\infty f_{\gamma|w}(\gamma;w) f_w(w) dw \text{ .... (14)}$$

where $w = \xi^2$ and $f_{\gamma|w}(\gamma;w)$ is obtained from (16) when rms power of the signal components is shadowed, given as

$$f_{\gamma|w}(\gamma;w) = \frac{\mu^\mu(1+\kappa)^\mu(m_r-1)^{m_r}\Gamma(m_r+\mu)}{\Gamma(m_r)\Gamma(\mu)(\mu\kappa+(m_r-1))^{m_r+\mu}}\frac{\gamma^{\mu-1}}{(w\bar{\gamma})^\mu} \text{ .... (15)}$$

On substituting (15) and $f_w(w) = \frac{m^m w^{m-1} e^{-mw}}{\Gamma(m)}$ into (14) and availing the relation given by [20, Eq. (3.381.4)], we get the origin PDF

$$f_\gamma(\gamma) \simeq \frac{m^\mu\mu^\mu(1+\kappa)^\mu(m_r-1)^{m_r}\Gamma(m_r+\mu)\Gamma(m-\mu)}{\Gamma(m)\Gamma(m_r)\Gamma(\mu)(\mu\kappa+(m_r-1))^{m_r+\mu}}\frac{\gamma^{\mu-1}}{\bar{\gamma}^\mu} \text{ .... (16)}$$

Similar to single shadowed $\kappa-\mu$ fading, the unified representation of double shadowed $\kappa-\mu$ fading will acquire a similar structure with the parameter $\hat{R}$ as defined in Table-2. With the exception of the single KMS Type-III and double KMS Type-III, where the condition $m > \mu$ must be satisfied, all other derived results remain applicable for arbitrary values of the fading parameters.

Table 2: Parameters for Origin κ−μ double shadowed family PDFs

Fading Types	$\hat{R}$
Double KMS Type-I	$\frac{\mu^\mu m^m(1+\kappa)^\mu\Gamma(m_r+\mu)}{\Gamma(\mu)\Gamma(m_r)(m+\mu\kappa)^m(m_r-1)^\mu}$

Double KMS Type-II	$\frac{\mu^{\mu}(1+\kappa)^{\mu}(m_r-1)^{m_r}\Gamma(\mu+m_r)}{\Gamma(\mu)\Gamma(m_r)\left(\frac{\mu\kappa}{m}\right)^{\mu+m}}\Psi\left(\mu+m_r,\mu+m_r-m+1;(m_r-1)\frac{m}{\mu\kappa}\right)$
Double KMS Type-III	$\frac{m^{\mu}\mu^{\mu}(1+\kappa)^{\mu}(m_r-1)^{m_r}\Gamma(m_r+\mu)\Gamma(m-\mu)}{\Gamma(m)\Gamma(m_r)\Gamma(\mu)(\mu\kappa+(m_r-1))^{m_r+\mu}}$

2.2.2.4 Origin PDF with SC

In the SC method, the diversity branch chosen by the receiver offers the largest SNR among the (L) branches. The CDF of the resulting SNR is therefore given by

$$F_{\gamma_{SC}}(\gamma) = \prod_{l=1}^{L} F_{\gamma_l}(\gamma) \quad (17)$$

where $F_{\gamma_l}(\gamma)$ is the CDF of the l-th branch and is derived from (2) by substituting it into $F_\gamma(\gamma) = \int_0^\gamma f_\gamma(\gamma)d\gamma$ and integrating it [20, Eq. (2.01.1)], we get

$$F_\gamma(\gamma) \simeq \frac{\hat{R}}{\mu\bar{\gamma}^{\mu}}\gamma^{\mu} \quad (18)$$

On substituting (23) into (22), we get

$$F_{\gamma_{SC}}^{inid}(\gamma) \simeq \prod_{l=1}^{L}\left(\frac{\hat{R}_l}{\mu_l\bar{\gamma}_l^{\mu_l}}\right)\gamma^{(\sum_{l=1}^{L}\mu_l+1)-1} \quad (19)$$

Further to derive the PDF expression, we differentiate (24) against γ, performing this differentiation produces the desired expression

$$f_{\gamma_{SC}}^{inid}(\gamma) \simeq \left(\sum_{l=1}^{L}\mu_l\right)\prod_{l=1}^{L}\left(\frac{\hat{R}_l}{\mu_l\bar{\gamma}_l^{\mu_l}}\right)\gamma^{(\sum_{l=1}^{L}\mu_l)-1} \quad (20)$$

Assuming i.i.d., the PDF expression is given as

$$f_{\gamma_{SC}}^{iid}(\gamma) = L\frac{\hat{R}^L}{\mu^{L-1}\bar{\gamma}^{L\mu}}\gamma^{L\mu-1} \quad (21)$$

2.2.3 Unified Origin PDF

A unified origin PDF representation can be formulated by expressing the statistical behavior of Unified representation of the PDF in the neighborhood of the origin can be provided based on the modeling of the statistical properties of independent random variables by means of a unified analytical expression. Instead of dealing separately with each distribution, the suggested approach involves the representation of the distributions under consideration as special cases of a unified general model. The unified PDF representation in the neighborhood of the origin is thus given by

$$f_\gamma(\gamma) \simeq \frac{\boldsymbol{R}_\chi}{\bar{\gamma}^{\Xi_\chi}}\gamma^{\boldsymbol{\Omega}_\chi-1}\} \quad (22)$$

where parameters $\boldsymbol{R}_\chi$, $\boldsymbol{\Xi}_\chi$, and $\boldsymbol{\Omega}_\chi$ for i.n.i.d. and i.i.d. cases are defined in the Table 3 with the exception for i.i.d case that $\bar{\gamma}_1 = \bar{\gamma}_2 = \cdots = \bar{\gamma}$.

Table 3: Parameters for generalized PDF around origin single and double shadowed κ μ family

Diversity		Single and Double shadowed $\kappa-\bar{\mu}$	
		i.n.i.d.	i.i.d.
SC	$\boldsymbol{R}_\chi$	$\left(\sum_{l=1}^{L}\mu_l\right)\prod_{l=1}^{L}\left(\frac{\hat{R}_l}{\mu_l}\right)$	$L\frac{\hat{R}^L}{\mu^{L-1}}$
	$\boldsymbol{\Xi}_\chi$	$\sum_{l=1}^{L}\mu_l$	$L\mu$

	$\boldsymbol{\Omega}_{\chi}$	$\sum_{l=1}^{L} \mu_l$	$L\mu$

3. Short Packet Performance Analysis

The Applications in 5G-and-beyond era, such as machine-to-machine (M2M), device-to-device (D2D), and Internet of Things (IoT) communications, require not only ultra-low latency but also high reliability of transmission [22]–[24]. Short-packet communication becomes one of the key enabling technologies in order to meet the above-mentioned requirements due to the possibility of fast and efficient transfer of small-size data packets. The decrease of packet size helps to reduce the delay of communication; thus, this paradigm is quite appropriate for time-sensitive services in the next generation of wireless networks. Since short-packet communication systems are intended to ensure reliable transmission of data under severe conditions of delay limitations, the analysis of the communication system in this section is carried out in the context of finite block-length (FBL) paradigm. Unlike asymptotic information theory, the FBL approach is based on the practical trade-off between transmission rate, packet length, and decoding performance under the limitation of the number of channels uses [25]. Thus, the average block error rate (BLER) and delay outage rate (DOR) are chosen as the main performance criteria for the analyzed communication system.

3.1 Average BLER

The Average BLER is the likelihood that the transmitted block will not be successfully decoded. BLER is one of the most important metrics when it comes to measuring communication reliability, especially in wireless systems which operate in the framework of the finite blocklength (FBL) regime [26]. For the AWGN channel, the average BLER can be calculated with the help of the proven analytical formula presented in [24, Eq. (27)]:

$$BLER(\gamma) \simeq \begin{cases} 1, \gamma \leq \xi \\ \frac{1}{2} - \frac{\delta}{\sqrt{2\pi}}(\gamma - n), \xi < \gamma < \nu \\ 0, \gamma \geq \nu \end{cases} \quad \text{(23)}$$

where $\xi = \hat{n} - \sqrt{\frac{\pi}{2\delta^2}}$, $\nu = \hat{n} + \sqrt{\frac{\pi}{2\delta^2}}$, $\hat{n} = 2^{\frac{K}{L}} - 1$, $\delta = \sqrt{\frac{L}{2\pi}}\left(2^{\frac{2K}{L}} - 1\right)^{-\frac{1}{2}}$, where N is the block-length and K represents the number of information bits within each block. In fading scenarios, the average BLER for FBL transmission is articulated as

$$\bar{A}_{BLER} \simeq \int_0^{\infty} BLER(\gamma) f_{\gamma}(\gamma) d\gamma \quad \text{(24)}$$

Further, substituting (22) into (23), and after mathematical simplification, we get

$$\bar{A}_{BLER} \simeq \underbrace{\int_0^{\xi} f_Y(\gamma) d\gamma}_{I_1} - \underbrace{\frac{\delta}{\sqrt{2\pi}} \int_{\xi}^{\nu} \gamma f_Y(\gamma) d\gamma}_{I_2} + \underbrace{\left(\frac{1}{2} + \frac{\delta\hat{\eta}}{\sqrt{2\pi}}\right) \int_{\xi}^{\nu} f_Y(\gamma) d\gamma}_{I_3} \quad \text{(25)}$$

Putting (22) into (25), I_1, I_2, and I_3 are expressed as

$$I_1 = \frac{\boldsymbol{R}_{\chi}}{\bar{\gamma}^{\boldsymbol{\Xi}_{\chi}}} \int_0^{\xi} \gamma^{\boldsymbol{\Omega}_{\chi}-1} d\gamma \quad \text{(26)}$$

$$I_2 = \frac{\delta}{\sqrt{2\pi}} \frac{\boldsymbol{R}_{\chi}}{\bar{\gamma}^{\boldsymbol{\Xi}_{\chi}}} \int_{\xi}^{\nu} \gamma^{\boldsymbol{\Omega}_{\chi}} d\gamma \quad \text{(27)}$$

$$I_3 = \left(\frac{1}{2} + \frac{\delta\hat{\eta}}{\sqrt{2\pi}}\right) \frac{\boldsymbol{R}_{\chi}}{\bar{\gamma}^{\boldsymbol{\Xi}_{\chi}}} \int_{\xi}^{\nu} \gamma^{\boldsymbol{\Omega}_{\chi}-1} d\gamma \quad \text{(28)}$$

Utilizing [20, Eq. (2.01.1)], we get the solution for I_1, I_2, and I_3 given as

$$I_1 = \frac{\boldsymbol{R}_{\chi}}{\bar{\gamma}^{\boldsymbol{\Xi}_{\chi}}} \frac{\xi^{\boldsymbol{\Omega}_{\chi}}}{\boldsymbol{\Omega}_{\chi}} \quad \text{(29)}$$

$$I_2 = \frac{\delta}{\sqrt{2\pi}} \frac{\boldsymbol{R}_{\chi}}{\bar{\gamma}^{\boldsymbol{\Xi}_{\chi}}} \frac{\nu^{\boldsymbol{\Omega}_{\chi}+1} - \xi^{\boldsymbol{\Omega}_{\chi}+1}}{\boldsymbol{\Omega}_{\chi}+1} \quad \text{(30)}$$

$$I_3 = \left(\frac{1}{2} + \frac{\delta\hat{\eta}}{\sqrt{2\pi}}\right) \frac{\boldsymbol{R}_{\chi}}{\bar{\gamma}^{\boldsymbol{\Xi}_{\chi}}} \frac{\nu^{\boldsymbol{\Omega}_{\chi}} - \xi^{\boldsymbol{\Omega}_{\chi}}}{\boldsymbol{\Omega}_{\chi}} \quad \text{(31)}$$

Further, substituting (29), (30), and (31) into (25), we get the asymptotic solution for the average BLER

$$\bar{A}_{BLER} \simeq \frac{\boldsymbol{R}_{\mathcal{X}}}{\bar{\gamma}^{\Xi_{\mathcal{X}}}}\left[\frac{\xi^{\boldsymbol{\Omega}_{\mathcal{X}}}}{\boldsymbol{\Omega}_{\mathcal{X}}} - \frac{\delta}{\sqrt{2\pi}}\frac{\nu^{\boldsymbol{\Omega}_{\mathcal{X}}+1} - \xi^{\boldsymbol{\Omega}_{\mathcal{X}}+1}}{\boldsymbol{\Omega}_{\mathcal{X}}+1} + \left(\frac{1}{2} + \frac{\delta\hat{\eta}}{\sqrt{2\pi}}\right)\frac{\nu^{\boldsymbol{\Omega}_{\mathcal{X}}} - \xi^{\boldsymbol{\Omega}_{\mathcal{X}}}}{\boldsymbol{\Omega}_{\mathcal{X}}}\right] \ldots\ldots\ldots\ldots\ldots (32)$$

3.2 Delay Outage Rate

The Delay Outage Rate (DOR) is another metric which is widely used in short-packet communication systems. It can be defined as the likelihood of the event in which the time of successful transmission of the data packet ($\mathcal{DT}_{ora}$) surpasses the predefined threshold value. Thus, DOR gives us an effective tool to determine whether or not our communication system meets the desired latency and reliability criteria. Assuming an optimal rate adaptation and a short-sized data packet (H), the DOR can be represented as [27, Eqs. (2)–(3)]

$$DOR_{ora} = Pr[\mathcal{DT}_{ora} > \mathcal{T}_{th}] = Pr\left[\frac{H}{B\log_2(1+\gamma)} > \mathcal{T}_{th}\right] \ldots\ldots\ldots\ldots\ldots (33)$$

where $P_r[.]$ denotes the probability measure, and B is the transmission bandwidth. The mathematical relation given in (33) is re-expressed as

$$DOR_{ora} = Pr[\gamma < \mathcal{Y}_{th}] = \int_0^{\mathcal{Y}_{th}} f_\gamma(\gamma)d\gamma \ldots\ldots\ldots\ldots\ldots (34)$$

where $\mathcal{Y}_{th} = 2^{\frac{H}{B\mathcal{T}_{th}}} - 1$. On substituting (22) into (34), the solution for the integral of DOR_{ora} is given by

$$DOR_{ora} \approx \frac{\boldsymbol{R}_{\mathcal{X}}}{\bar{\gamma}^{\Xi_{\mathcal{X}}}\boldsymbol{\Omega}_{\mathcal{X}}}\mathcal{Y}_{th}^{\boldsymbol{\Omega}_{\mathcal{X}}} \ldots\ldots\ldots\ldots\ldots (35)$$

4. Diversity and SNR Gains

The diversity gain and SNR gain play an essential role as the performance metrics of high SNR behavior of the diversity-based communication system. While the diversity gain is related to the slope of the asymptotic performance curve and is proportional to the rate of decrease of the outage probability versus increase of the average SNR, the SNR gain denotes the horizontal shift of the performance curve relative to the reference system. In other words, it shows the performance gain of the system compared to the reference one with unchanged asymptotic slope [18], [19], [28]. As a consequence, the obtained asymptotic expressions could be rewritten in terms of the diversity and SNR gain as follows:

$$\mathcal{B} = (\mathcal{G}^c\bar{\gamma})^{-\mathcal{G}^d}, \quad \mathcal{B} \in \{\bar{A}_{BLER}, DOR_{ora}\} \ldots\ldots\ldots\ldots\ldots (36)$$

in which SNR gain and diversity gain are given by $\mathcal{G}^c$ and $\mathcal{G}^d$, respectively. The value of $\mathcal{G}^c$ and $\mathcal{G}^d$ for the rate outage probability and the delay outage rate is given below:

Average BLER

$$\mathcal{G}^c = \left(\boldsymbol{R}_{\mathcal{X}}\left[\frac{\xi^{\boldsymbol{\Omega}_{\mathcal{X}}}}{\boldsymbol{\Omega}_{\mathcal{X}}} - \frac{\delta}{\sqrt{2\pi}}\frac{\nu^{\boldsymbol{\Omega}_{\mathcal{X}}+1} - \xi^{\boldsymbol{\Omega}_{\mathcal{X}}+1}}{\boldsymbol{\Omega}_{\mathcal{X}}+1} + \left(\frac{1}{2} + \frac{\delta\hat{\eta}}{\sqrt{2\pi}}\right)\frac{\nu^{\boldsymbol{\Omega}_{\mathcal{X}}} - \xi^{\boldsymbol{\Omega}_{\mathcal{X}}}}{\boldsymbol{\Omega}_{\mathcal{X}}}\right]\right)^{-\frac{1}{\Xi_{\mathcal{X}}}} \text{ and } \mathcal{G}^d = \Xi_{\mathcal{X}}.$$

Delay outage rate

$$\mathcal{G}^c = \left(\frac{\boldsymbol{R}_{\mathcal{X}}\mathcal{Y}_{th}^{\boldsymbol{\Omega}_{\mathcal{X}}}}{\boldsymbol{\Omega}_{\mathcal{X}}}\right)^{-\frac{1}{\Xi_{\mathcal{X}}}} \quad \text{and} \quad \mathcal{G}^d = \Xi_{\mathcal{X}}.$$

These results indicate that diversity gain is solely determined by the multipath parameter μ and diversity order L.

5. Discussion on Performance Evaluation

In this section, the numerical results are provided for verifying the analytic formulas derived in Section III for the average BLER and DOR. The obtained closed-form expressions in (32) and (35) give a unified framework applicable to both i.n.i.d. and i.i.d. channel model by choosing the proper set of parameters $\boldsymbol{R}_{\mathcal{X}}$, $\Xi_{\mathcal{X}}$, and $\boldsymbol{\Omega}_{\mathcal{X}}$ listed in Table III. Unless stated otherwise, the numeric values are derived assuming i.i.d. fading channels to allow easy understanding of the analysis results along with the trends in performance. Monte Carlo simulations are carried out to confirm the analysis results using more than 10^6 channel realizations. This number is used to increase the accuracy of the simulation results as well as minimize the estimation error.

In order to investigate the impact of various shadowing scenarios, the average BLER values in the case of double KMS Type-I, Type-II, and Type-III fading channels are shown in Fig. 1. In addition, the dependence between the number of information bits and reliability of transmissions with finite blocks of data is demonstrated. For simulation purposes, $\kappa = 1$, $\mu = 1$, $m = 1.2$, and $m_r = 1.4$ are used, and the value of the blocklength is equal to (N=500). The average BLERs for the selected fading channels are the minimum for double KMS Type-II fading, next is Type-III, and Type-I. Furthermore, with the increase in the number of information bits, the BLERs become larger. This happens due to the increased value of the coding rate.

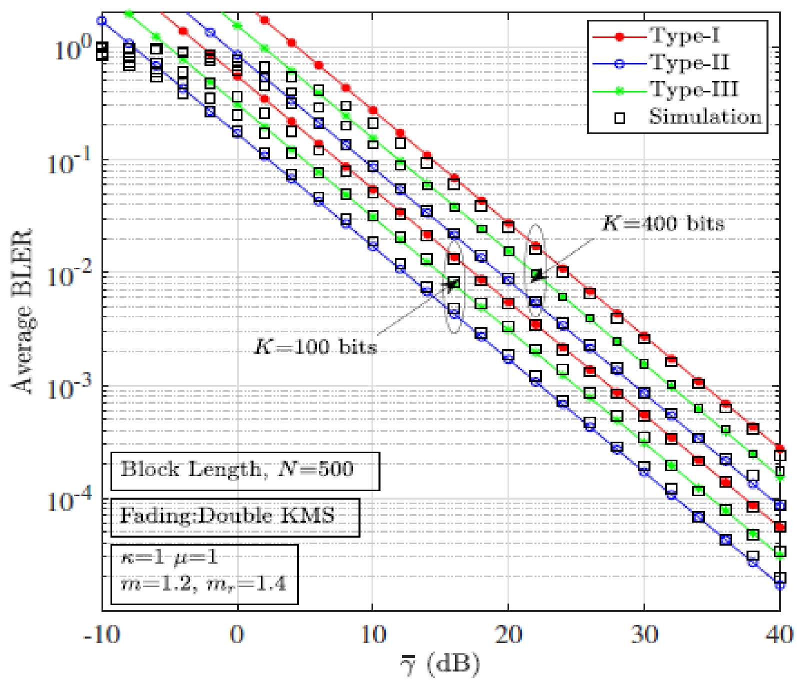

Fig. 1 Average BLER for double KMS Type-I, Type-II, and Type-III with varying K.

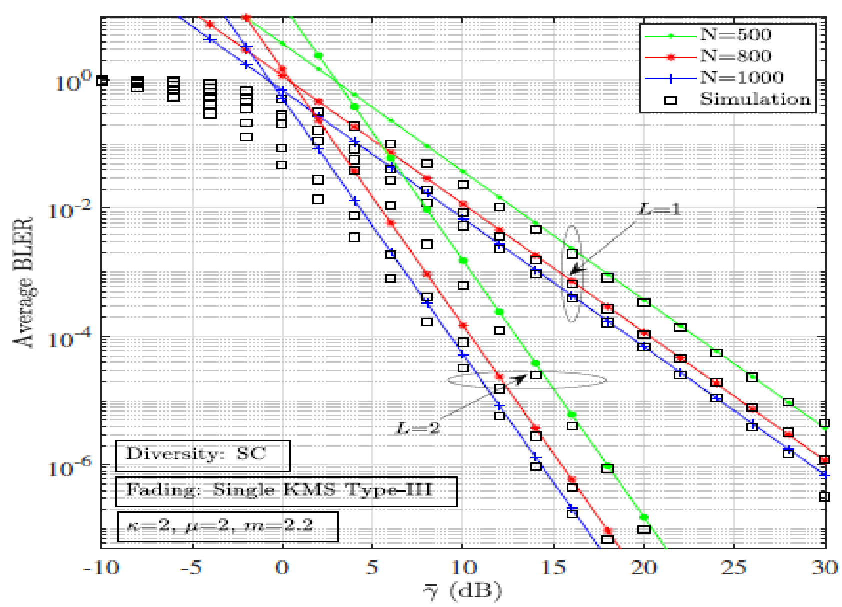

Fig. 2 Average BLER for single KMS Type-III with SC diversity and varying N.

Figure 2 shows the impact of diversity order and block length on the BLER performance in single KMS Type-III fading. From Fig. 3, it can be seen that a longer block length results in an improved BLER performance. However, longer blocks can increase the communication latency due to the increase in the time needed to transmit them. Moreover, an increased diversity order improves the received SNR through several independently faded signal paths. The increased received SNR reduces the BLER. Hence, although both a longer block length and a higher diversity order result in good error performance, care should be taken when considering the added latency due to long block lengths.

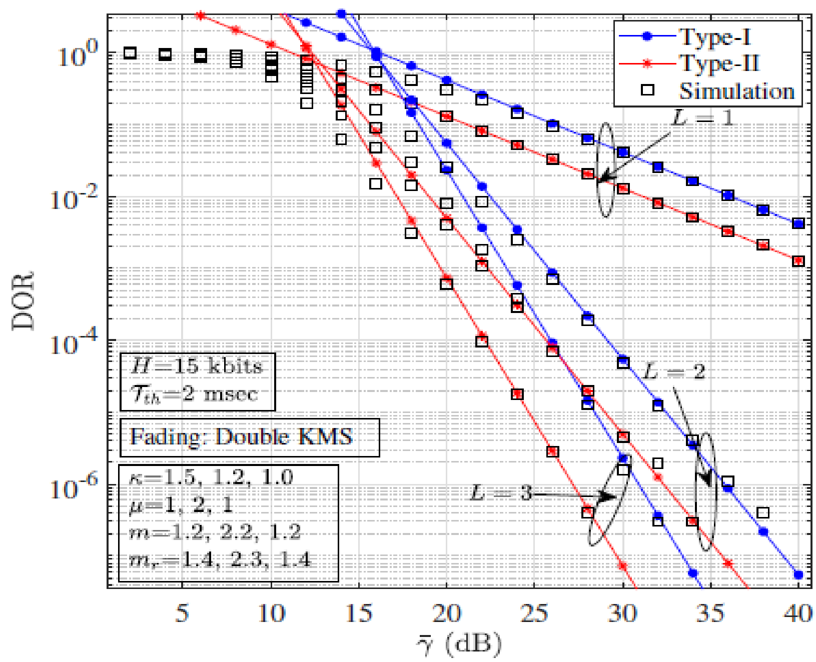

Fig. 3 DOR for double KMS Type-I and Type-II with SC diversity.

Figure 3 shows the performance impact of the double KMS Type-I and Type-II fading models on the DOR, taking into consideration the SC diversity over i.n.i.d. channels. Under similar fading and system parameters, the Type-II model shows better performance than the Type-I model in terms of having lower DOR. While it can be observed that the two fading models have almost similar slopes, meaning similar asymptotic behavior, the slope differs significantly with the diversity order, such that increasing the diversity order from (L=1) to (L=2) results in significant improvements in the performance, and further increases in the diversity order result in marginal gains. This can be explained by the fact that adding the first extra diversity branch reduces the impact of deep fading significantly, while the gain from further diversity branches diminishes.

For instance, at $\bar{\gamma} = 20$ (dB)average SNR, the DOR for Type-I fading is about 10^{-2} at (L=1), but it drops to almost $10^{-3}$for (L=2) and (L=3). However, in Type-II fading, the DOR is of the order of 10^{-2}at (L=1), but is reduced to $10^{-3}$and 10^{-4} at (L=2) and (L=3), respectively. In addition to this, the results confirm that raising the diversity order to (L=2), compared with (L=1), results in a large horizontal shift in the DOR curves, which correspond to a gain of more than *15* (dB) in SNR. However, the increase in the diversity order from (L=2) to (L=3) does not bring significant benefits, leading to a relatively low gain of around 3 (dB).

6. Conclusion

In this paper, an asymptotic analysis of the κ-μ/shadowed fading family under three different scenarios including single and double shadowing is performed. To ensure higher reliability in the system, spatial diversity is used with SC that leads to SNR improvement. First of all, the PDF near the origin is found for the single- and double-shadowed KMS fading models. After that, the obtained results are generalized to find the corresponding PDFs in the case of diversity-assisted communication systems. Based on the statistical model derived in this paper, asymptotic formulas are found for several SPC performance measures such as the average BLER and DOR. Obtained results give valuable information on how the average SNR and diversity gain influence the behavior of these performance metrics.

In addition, it can be seen that the diversity gain depends only on the number of diversity branches and multipath clusters. Finally, Monte Carlo simulations are used to validate the theoretical results.

Acknowledgements Manuscript communication number: IU/R&D/2026-MCN0004840, Integral University Lucknow. The authors would like to extend their most sincere gratitude to the editors as well as the reviewers who remained anonymous for their informative reviews and remarks.

Declaration: All the authors have collectively contributed to this manuscript. All authors have reviewed and endorsed the final version of the manuscript.

Funding: No financial support was received for this research endeavors.
Data Availability: N/A

Code Availability: N/A

Conflicts of Interest: There are no conflicts of interest present.

References

1. L. Tejerina, G.R., Silva, C.R.N., Souza, R.A.A., Yacoub, M.D. 2023. "On the Extended η-μ Model: New Results and Applications to IRS-Aided Systems." IEEE Trans. Veh. Technol. 72 (4): 4133–42. DOI: 10.1109/TVT.2022.3222064
2. Ahmad, S., Khan, I.U., Khan, M.J. 2023. "Performance analysis of NOMA based UAV-assisted cooperative relaying system with direct link over Rician fading channels." Eng. Res. Express, 5: 1–20. DOI: 10.1088/2631-8695/acf7f2
3. Zheng, J., Wu, T., Lai, X., Pan, C., Elkashlan, M., Wong, K.K. 2024. "FAS-assisted NOMA short-packet communication systems." IEEE Trans. Veh. Technol. 73 (7): 10732–37. DOI: 10.1109/TVT.2024.3363115f
4. Giordani, M., Polese, M., Mezzavilla, M., Rangan, S., Zorzi, M. 2020. "Toward 6G networks: Use cases and technologies." IEEE Commun. Mag. 58 (3): 55–61. DOI: 10.1109/MCOM.001.1900411
5. Srinivasarao, K., Rao, V.V., Sharma, P. 2025. "Outage analysis of IRS-NOMA system over η-μ fading channel" Int. J. Sens. Wireless Commun. Control, 15 (1), 58–63. https://doi.org/10.2174/0122103279312349240710060042.
6. Vo, D.T., Thi-Pham, T.H., Tran, M., Kim, B.S., Kharel, R., Voznak, M. 2025. "Short packet communication in IoT networks: Performance analysis." J. Inf. Telecommun. 10: 199-212, DOI: 10.1080/24751839.2025.2487353
7. Vu, T. -H., Nguyen, T. -V., Pham, Q. -V., Costa, D. B. da, Kim, S. 2023. "Short-Packet Communications for UAV-Based NOMA Systems Under Imperfect CSI and SIC," IEEE Trans. Cogn. Commun. Netw., 9 (2): 463-478. doi: 10.1109/TCCN.2022.3225118.
8. Jain, A., Khan, I.U., Chauhan, P.S., Bhatia, V. 2026. "SEP Analysis on the Shadowed Beaulieu-Xie and Extended η-μ Fadings in Additive Laplacian Noise." Wireless Pers. Commun. 146: 1499–1520, DOI: 10.1007/s11277-026-11930-8
9. Paris, J.F. 2014. "Statistical Characterization of κ-μ Shadowed Fading." IEEE Trans. Veh. Technol. 63 (2): 518–26. DOI: 10.1109/TVT.2013.2281198
10. Moreno-Pozas, L., Lopez-Martinez, F.J., Paris, J.F., Martos-Naya, E. 2016. "The κ–μ Shadowed Fading Model: Unifying the κ – μ and η – μ Distributions." IEEE Trans. Veh. Technol. 65 (12): 9630–41. DOI: 10.1109/TVT.2016.2549523
11. ElHalawany, B.M., Jameel, F., Costa, D.B., Dias, U.S., Wu, K. 2020. "Performance Analysis of Downlink NOMA Systems over κ - μ Shadowed Fading Channels." IEEE Trans. Veh. Techno. 69 (1): 1046–50. DOI: 10.1109/TVT.2019.2953804
12. Chauhan, P.S., Sau, P.C., Kumar, S., A¨ıssa, S., Badarneh, O.S., Bhatia, V. 2025. "Analyzing Multi-Antenna Wireless Systems: Distribution Functions, Integral Identities, and Performance Metrics." IEEE Trans. Veh. Technol. 74 (12): 18930–41. DOI: 10.1109/TVT.2025.3583346
13. Simmons, N., Da Silva, C.R.N., Cotton, S.L., Sofotasios, P.C., Yoo, S.K., Yacoub, M.D.2020. "On Shadowing the κ-μ Fading Model." IEEE Access 8: 120513–120536. DOI: 10.1109/ACCESS.2020.3003218
14. Chauhan, P.S., Sau, P.C., Kumar, S., Jain, A., Bhatia, V. 2025. "SEP Analysis on the κ − μ Shadowed Fading with Additive Laplacian Noise." Dig. Signal Process. 161: 105135. DOI: 10.1016/j.dsp.2025.105135
15. Simmons, N., Silva, C.R., Cotton, S.L., Sofotasios, P.C., Ki Yoo, S., Yacoub, M.D. 2019. "The Double Shadowed κ-μ Fading Model." Proc. Int. Conf. Wireless Mobile Comput., Netw. Commun. (WiMob), 1–6, Barcelona, Spain. DOI: 10.1109/WiMOB.2019.8923336
16. Singh, R., Rawat, M. 2019. "On the Performance Analysis of Effective Capacity of Double Shadowed κ − μ Fading Channels." Proc. IEEE Reg. 10 Conf. (TENCON), 2019, 806–10, Kochi, India. DOI: 10.1109/TENCON.2019.8929628
17. Singh, R., Rawat, M. 2019b. "Outage Analysis of Double Shadowed κ − μ Fading Channels." Proc. 10th Int. Conf. Comput., Commun. Netw. Technol. (ICCCNT 2019), 1–4. Kanpur, India, July 6-8, 2019, DOI: 10.1109/ICCCNT45670.2019.8944440
18. Chauhan, P.S., Kumar, S., Upaddhyay, V.K., et al. 2022. "Generalised Asymptotic Framework for Double Shadowed Fading with Application to Wireless Communication and Diversity Reception." Wireless Netw. 28: 1923–34. DOI: 10.1007/s11276-021-02879-4
19. Wang, Z., Giannakis, G.B. 2003. "A Simple and General Parameterization Quantifying Performance in Fading Channels." IEEE Trans. Commun. 51 (8): 1389–98. DOI: 10.1109/TCOMM.2003.815053

20. Gradshteyn, I.S., Ryzhik, I.M. 2007. Table of Integrals, Series, and Products. 7th ed. Academic Press, Inc., San Diego, CA, USA.
21. Prudnikov, A.P., Brychkov, Y.A., Marichev, O.I. 1986. Integrals and Series, Volume 1: Elementary Functions.Gordon and Breach Science Publishers,New York.
22. Sun, X., Yan, S., Yang, N., Ding, Z., Shen, C., Zhong, Z. 2018. "Short-packet downlink transmission with non-orthogonal multiple access." IEEE Trans. Wireless Commun. 17 (7): 4550–64. DOI: 10.1109/TWC.2018.2812874
23. Yu, Y., Chen, H., Li, Y., Ding, Z., Vucetic, B. 2018. "On the performance of non-orthogonal multiple access in short-packet communications." IEEE Commun. Lett. 22 (3): 590–93. DOI: 10.1109/LCOMM.2018.2792047
24. Ad, M., Khelil, A. 2025. "BER analysis of underlay cooperative cognitive radio-based NOMA system" Int. J. Sens. Wireless Commun. Control, 15 (3), e22103279275260. https://doi.org/10.2174/0122103279275260240925050941
25. Polyanskiy, Y., Poor, H.V., Verd´u, S. 2010. "Channel coding rate in the finite blocklength regime." IEEE Trans. Inf. Theory 56 (5): 2307–59. DOI: 10.1109/TIT.2010.2043769
26. Lai, X., Wu, T., Zhang, Q., Qin, J. 2021. "Average Secure BLER Analysis of NOMA Downlink Short-Packet Communication Systems in Flat Rayleigh Fading Channels," IEEE Trans. Wireless Commun., 20 (5): 2948-2960. doi: 10.1109/TWC.2020.3045736
27. Yang, H.-C., Choi, S., Alouini, M.-S. 2020. "Ultra-Reliable Low-Latency Transmission of Small Data over Fading Channels: A Data-Oriented Analysis." IEEE Commun. Lett. 24 (3): 515–19. DOI: 10.1109/LCOMM.2020.2965958
28. Chauhan, P.S., Kumar, S., Jain, A., Hanzo, L. 2023. "An Asymptotic Framework for Fox's H-Fading Channel with Application to Diversity-Combining Receivers." IEEE Open J. Veh. Technol. 4: 404–16. DOI: 10.1109/OJVT.2023.3267972